

ATTEMPTING OF BRAIN TUMOR CLASSIFICATION ON DENSE NET AND RECURRENT NEURAL NETWORK FRAMENTS

Sachin Gautam

ABSTRACT

We present a comprehensive Braintumors screening and arrangement strategy for identifying and recognizing different kinds of cerebrum tumors on MR pictures. The difficulties emerge from the unique varieties of area, shape, size, and complexity of these tumors. The proposed calculations begin with highlight extraction from pivotal cuts utilizing thick convolutional neural systems; the acquired following highlights of many edges are then bolstered into a broken neural network for grouping. Unique concerning most other cerebrum tumor grouping calculations, our structure is free from the manual or programmed locale of interests division. The outcomes gave an account of an open dataset, and a populace of 422 exclusive MRI checks analyzed as should be expected, gliomas, meningiomas, and metastatic cerebrum tumors exhibit the adequacy and effectiveness of our technique.

1. INTRODUCTION

Brian tumor is a standout amongst the most lethal malignant growths. In the United States, an expected 700,000 individuals are living with essential mind and focal sensory system tumors. Almost 80,000 new instances of primary cerebrum tumors are analyzed yearly, and around 33% are threatening [1]. A wide range of kinds of mind tumors exist. The most common cerebrum tumor types in grown-ups are gliomas and meningiomas.

Therapeutic imaging assumes a focal job in diagnosing mind tumors. Many imaging modalities can give data about mind tissue non-intrusively, for example, MRI, CT, and PET. X-ray has primarily been utilized. Y. Zhou, Z. Li and Hong Zhu are similarly contributed to co-first creators; Kai Xu and Jinhui Xu are co-relating creators. As often as possible in mind tumor recognition and distinguishing proof, because of its high differentiation of delicate tissue, lofty spatial goals and free of radiation. Regardless of these actualities, mind tumor analysis remains a testing errand. PC Aided Diagnosis (CAD) can give enormous help in cerebrum tumor conclusion, forecast, and medical procedure. A run of the mill cerebrum tumor CAD framework comprises of three principal stages, tumor district of intrigue (ROI) division, including extraction, and arrangement (because of the separated highlights) [4,6,5]. Cerebrum tumor division, either manual or programmed, is maybe the most critical and tedious period of such a framework. A lot of exertion has been given to this issue, e.g., discharging openly available benchmark datasets and sorting out difficulties [10]. Numerous calculations have been proposed to take care of the cerebrum tumor division issue, for example, Deep Neural Networks [7] and SVM with Conditional Random Field [3]. Arrangements dependent on SVM or potentially ANN are then pursued to recognize unique kinds of mind tumors dependent on the extricated highlights from

ROIs. An essential impediment of such systems is the need for following ROIs, which can cause a couple of issues. Right off the bat, since mind tumors can shift significantly in their shapes, sizes, and areas, following ROIs could be very testing and regularly not wholly programmed. This may make noteworthy blunders the division, and be aggregated into the accompanying stages, along these lines prompting wrong grouping. Also, the tumor-encompassing tissues are recommended to be discriminative between various tumor classes [5]. Thirdly, depending entirely on the highlights of ROIs, implies finish numbness of the area data of the tumors, which can influence the arrangement impressively. The previously mentioned issues inspire us to propose an elective methodology for mind tumor screening and order, taking out the division stage. Mainly, we recommend to utilize the all-encompassing 3D pictures straightforwardly without the point by point explanation at the pixel or cut dimensions — our methodology models the 3D all-encompassing views as groupings of 2D cuts. It initially embraces an auto-encoder, in light of a profound DenseNet, to extricate highlights of each 2D image. This enables us to abstain from utilizing the first boisterous and high dimensional information. After highlights of 2D cuts separated, it is normal to apply an RNN, notably the LSTM model to deal with the successive information for the order. We likewise apply a convolutional display for successive information, by loading 2D cuts. This is propelled by ongoing work of utilizing simply convolutional auto-encoder for arrangement portrayal learning [12].

– The proposed models just need the all-encompassing name of patients other than pixel-wise/cut insightful marking. All-encompassing marks are a lot less demanding to get in daily clinical practice.

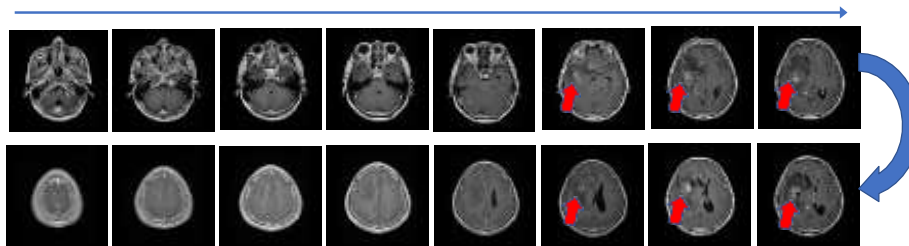


Fig. 1. An MR image sequence of a glioma patient.

We have gathered a dataset of 422 MRI examines, containing typical control pictures and also three sorts of mind tumors (i.e., meningioma, glioma, and metastasis tumor).

Our profound neural system executes a novel design, regarding 3D information as to arrangements of 2D cuts, and utilizing CNN &RNN to train succession to-mark mapping, with a DenseNet based auto-encoder for highlight extraction. Two proposed models DenseNet-LSTM and DenseNet which are shown with two analyses of tumor screening &type analyzing utilizing both open and exclusive datasets.

2 PRELIMINARIES

2.1 Brain-Tumor Image Representations

Mind tumors are generally determined to have MRI or CT pictures, where persistent I am spoken to by an arrangement of 2-D images, meaning as $X_i = \{x, \cdot, x\}$ with $X(i) \in \mathbb{R}^{A_1 \times A_2}$ being the outline picture. Not the same as existing mark through datasets where every 2-D view is related with a name, in our dataset, each succession of pictures X_i is associated with a single name $Y_i \in \{0, 1, P\}$, where P is the number of tumor types. Thus, our dataset is spoken to as $D = \{(X_i, Y_i)\}_N$ with N being the aggregate number of picture arrangements (counting Patients and ordinary individuals). Fig. 1 shows a model grouping of MRI pictures from a Glioma persistent in our particular dataset. Note that there are just a couple of edges demonstrating the presence of Glioma.

2.2 DenseNet

DenseNet [9] is an as of late proposed unique kind of convolutional neural systems, where the entirety of its past layers associates the current layer. The structure then anonymized prohibitive dataset will be shared transparently with imprints later on.

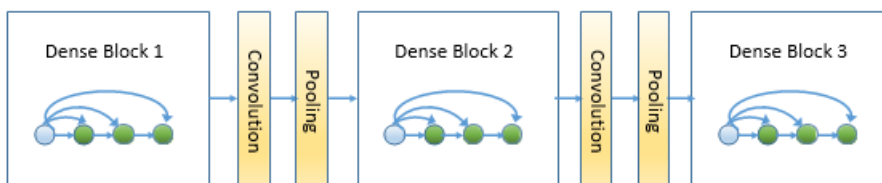


Fig. 2. A Deep DenseNet with three thick squares. In each solid square, the contribution for a specific layer is the link of all yields from its past layers; the return is acquired by convolving the grant with a few bits to be educated a few favorable circumstances over existing structures, for example, lightening the vanishing-slope issue, reinforcing highlight spread, empowering highlight reuse, and lessening the number of parameters. A profound DenseNet is characterized as an arrangement of DenseNets (called thick squares) associated successively, with extra convolutional and pooling activities between back to back thick squares. By such a development, we can fabricate a profound neural system sufficiently adaptable to speak to entangled changes. A case of the profound DenseNet is represented in Fig. 2.

2.3 RNN

RNN is an incredible casing work to show succession to-grouping information. In our Glioma cerebrum tumor application, the information succession corresponds to highlights of the MRI pictures, which are extracted with a DenseNet depicted over; the out-put arrangement ruffians to

a solitary mark, indicating whether the input grouping is diagnosed as a tumor or not. In particular, consider an information succession $X = x_1, \dots, x_T$, where x_t is the info information vector at

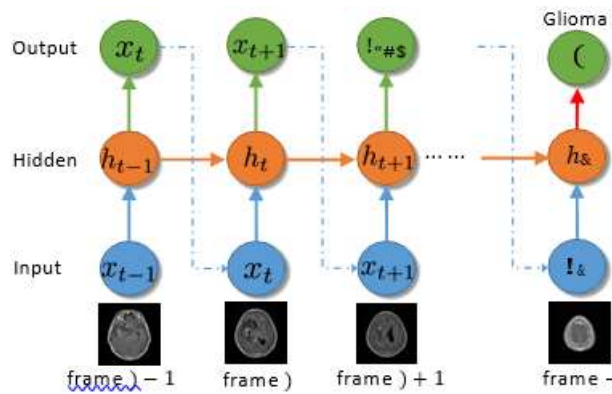


Fig. 3. The RNN structure.

Time t . The relating concealed state vector h_t at each time t is recursively ascertained by applying for a progressing work $h_t = (h_{t-1}, x_t)$ (indicated underneath). At long last, the yield y is determined by mapping the last state h_T to the namespace. Fig. 3 shows the RNN structure in our setting. Long Short-Term Memory (LSTM) Vanilla RNN characterizes as a straight transformation pursued by an initiation work. This basic structure can't demonstrate long haul reliance from the contribution, similar to the case in our application. Instead, we receive the more ground-breaking LSTM change work by presenting a memory cell that can save the state over significant lots [8]. In particular, each LSTM unit contains a cell c_t at time t , which can be seen as a memory unit. Perusing or composing the cell is controlled through sigmoid doors: input entryway i_t , overlook door f_t , and yield entryway o_t . Like this, the shrouded units h_t are refreshed as:

$$\begin{aligned}
 i_t &= \sigma(W_i x_t + U_i h_{t-1} + b_i), & f_t &= \sigma(W_f x_t + U_f h_{t-1} + b_f), \\
 o_t &= \sigma(W_o x_t + U_o h_{t-1} + b_o), & \tilde{c}_t &= \tanh(W_c x_t + U_c h_{t-1} + b_c), \\
 c_t &= f_t \odot c_{t-1} + i_t \odot \tilde{c}_t, & h_t &= o_t \odot \tanh(c_t)
 \end{aligned}$$

Where $\sigma(\cdot)$ Signifies the calculated sigmoid capacity and \odot speaks to the component savvy framework augmentation administrator. $W\{i,f,o,c\}$, $U\{i,f,o,c\}$ and $b_{i,f,o,c}$ are the weights of the LSTM to be scholarly. Having acquired the shrouded unit for the

last time step T , we delineate to y by essentially utilizing a direct change pursued by a softmax-layer, i.e., $p(y = k|h_T) = \text{Softmax}_k(W_y h_T + b_y)$, where $\text{Softmax}_k(a) = \frac{\exp(a_k)}{\sum_i \exp(a_i)}$, and W_y and b_y are the parameters to be scholarly.

Without three labeling Brain-Tumor Classification

We portray our model depends on the above building squares. Unique about existing techniques for tumor grouping utilizing a standard alone CNN, we propose two models to anticipate picture arrangements straightforwardly, wholly dispensing with the tedious methodology of marking each edge autonomously, subsequently free of naming.

3.1 DenseNet-LSTM show

There are mostly two difficulties in our assignment: I) Directly utilizing CNN to handle picture groupings is wrong as CNN is initially intended for static information. Luckily, LSTM gives us an appropriate method to manage grouping information. Accordingly, we receive LSTM for picture arrangement order. ii) Directly nourishing unique picture arrangements to an RNN works inadequately because the first pictures are generally loud and high-dimensional.

To reduce this issue, we propose an auto-encoder structure dependent on the profound DenseNet to separate highlights of the first pictures. The highlights from the auto-encoder are then encouraged to an RNN for grouping. In particular, in an auto-encoder, one trains an encoder and a decoder together, to recreate the yield the equivalent as information. To prepare the auto-encoder given mind tumor pictures $(x(i))_{i,t}$, the goal is to limit the remaking blunder:

ENC() and DEC() indicate the encoder and decoder actualized by two profound DenseNets, separately. In the wake of preparing the auto-encoder, the separated highlights for every one of the pictures is then utilized as the info information to make an RNN classifier for all-encompassing cerebrum tumor characterization. We embrace the standard cross-entropy misfortune capacity to make the RNN. The entire structure is represented in Fig. 4. We indicate this model as DenseNet-LSTM.

3.2 DenseNet display

An elective method to RNN for succession classification found recently is to supplant the RNN with a CNN [12]. We stack the highlights of a tumor-grouping came back from the auto-encoder as a 2-D tensor, and regard it as info information to a second profound DenseNet for classification. Along these lines, the between casing connections is converted into section savvy relationships in a transgression gle 2-D tensor, which can be viably modeled by the convolutional administrator in a DensetNet. We indicate this model as DenseNet-DenseNet.

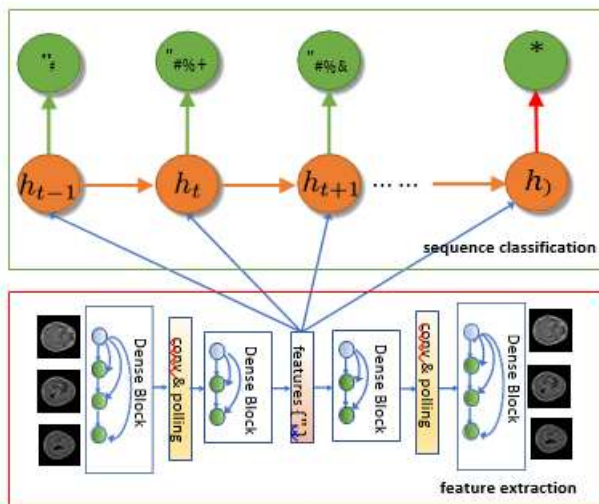


Fig. 4. The proposed DenseNet-LSTM model for labeling- free brain tumor classification.

4 EXPERIMENTS

The structure on two datasets, one open dataset and one restrictive dataset (gathered by our teammates in their healing center). We have two analyses to assess the proposed models: Tumor screening and tumor type order. Tumor screening is for trying the exactness of our methodology on choosing (or selection) regardless of whether a 2D arrangement picture contains a tumor. Tumor type characterization is to order tumors into various sorts.

Our usage depends on TensorFlow. To ease overfitting, we embrace the weight-rot regularization and dropout in the preparation. The auto-encoder part should be prepared just once. It takes around 5 hours for 10,000 cuts from 500 MRI groupings. The second part takes around 30 minutes for LSTM or one hour for DenseNet. The models were set up on an Nvidia Titan Xp GPU. For all he examinations, we heedlessly divide the dataset into a readiness dataset (72%), a test dataset (14%) and an endorsement dataset (14%). We reiterate this system for different occasions and report the mean and contrast of the exactnesses. Fig. 7 shows a couple of points of reference to desires to learn and adjust. More particular examination settings are given in the beneficial material. Open Dataset the general population dataset [5] incorporates 3064 (2D) cuts of cerebrum X-ray from 233 patients, containing 708 meningiomas, 1426 gliomas, and 930 pituitary tumors. Experienced radiologists physically outlined the tumors. Since our methodology does not rely upon division, we utilize only the widely inclusive characteristic of each slice to demonstrate the tumor type. Since this dataset does not have the course of action pictures required by our model, we convert each 2D see (cut) into a gathering of 20 cuts by either duplicating it on numerous occasions (for DenseNet-DenseNet) or including 19 zero grids (for DenseNet-LSTM). Our inspiration for using this dataset is for both approving the intensity of the proposed structure and achieving the best in class execution. In any case, our model isn't expected for managing such 2D datasets. Exclusive Dataset We have gathered a dataset of 422 MRI filters analyzed as would be expected (75), Glioma (150), meningiomas (67), and metastatic mind tumors (130). For every patient, T1, T2, and Flair MR pictures are accessible.

Test Setup In the DenseNet-based auto-encoder, for the encoder, it is a profound DenseNet with four thick squares. In each square, there are five convolutional layers with piece sizes of 3 and 1. We embrace similar arrangements for the decoder. For different parameters of the DenseNet, we welcome the default setting as in [9]. The element of the inert space for RNN is set to 128. Minibatch measure is set to 32. We utilize an approval set to choose the taking in rates from {1e-1, 1e-2, 1e-3, 1e-4, 1e-5}; the dropout rates for the information shrouded layer and each convolutional layer in the DenseNet from {0, 0.05, 0.1, 0.15, 0.2}, and the weight-rot rates from {1e-2, 1e-3, 1e-4, 1e-5}.

Tumor Screening people in the comprehensive dataset isn't reasonable for this errand since it just contains pictures with tumors. We assessed three models for tumor screening on the restrictive dataset: DenseNet-RNN (with vanilla RNN as a succession classifier), DenseNet-LSTM and DenseNet-DenseNet. Their exactnesses are 87.15% 3.79%, 91.09% 3.62%, 92.66% 2.73% individually. DenseNet-DenseNet presents the best execution for the restrictive dataset.

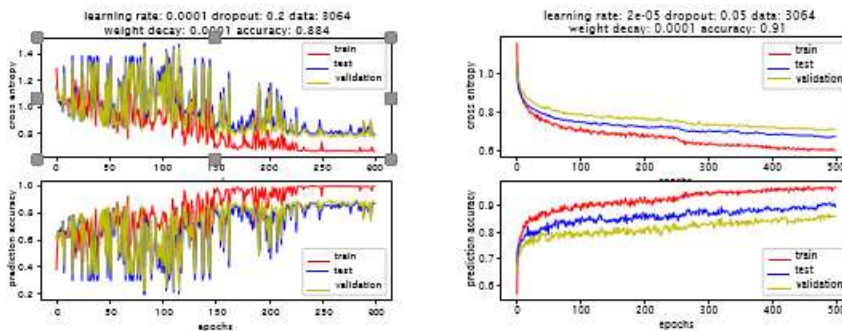


Fig. 5. Expectations to absorb information on open dataset. Left: tumor type classification with DenseNet-DenseNet. Right: tumor type grouping with DenseNet-LSTM.

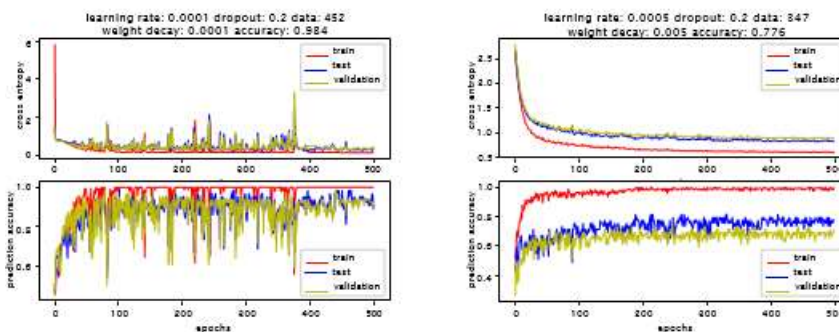


Fig. 6. Expectations to absorb information on restrictive dataset. Left: tumor screening with DenseNet-DenseNet. Right: tumor type grouping with DenseNet-LSTM.

Tumor Type Classification For people in general dataset, DenseNet-LSTM out-plays out all the past work on this dataset. The benchmark strategies [5] reports an exactness of 91.28% for its best

model dependent on an entangled element designing and additional information data (from pixel-wise marking). An ongoing model dependent on container systems [2] accomplishes 86.56% precision. Moreover, our models are substantially more powerful and valuable since they are intended to deal with 3D succession pictures and is without naming.

Our restrictive information is essentially more hard to learn that people in general one. Our DenseNet-LSTM is the best among different assortments. DenseNet-LSTM is likewise tried on one versus one tumor type arrangement, bringing about three gatherings of investigations. Table 1 condensed the outcomes. Fig. Seven and Fig. 6 demonstrates the expectations to absorb information of our models on the restrictive and open dataset, respectively.

Persistent embeddings with DenseNet and LSTM highlights: To represent how our proposed structure accomplishes high segregation capacity, we install the highlights from the DenseNet auto-encoder and the LSTM classifier onto a 2-D space, individually. Note that the highlights from the auto-encoder don't consider

Table 1. Summary of experimental results on tumor type classification.

Tumor type classification accuracies (three types)					
Models	DenseNet-RNN	DenseNet-LSTM	DenseNet-DenseNet	[5]	[2]
Public	84.61%± 1.87%	92.13%± 1.59%	86.68%± 1.54%	91.28%	86.56%
Proprietary	60.00%± 5.70%	71.10%± 3.82%	64.95%± 5.16%	-	-

Tumor type classification accuracies (two types) with DenseNet-LSTM			
	Glioma vs Meningiomas	Glioma vs Metastatic	Meningiomas vs Metastatic
Proprietary	80.83%± 6.65%	80.00%± 8.44%	82.50%± 4.18%

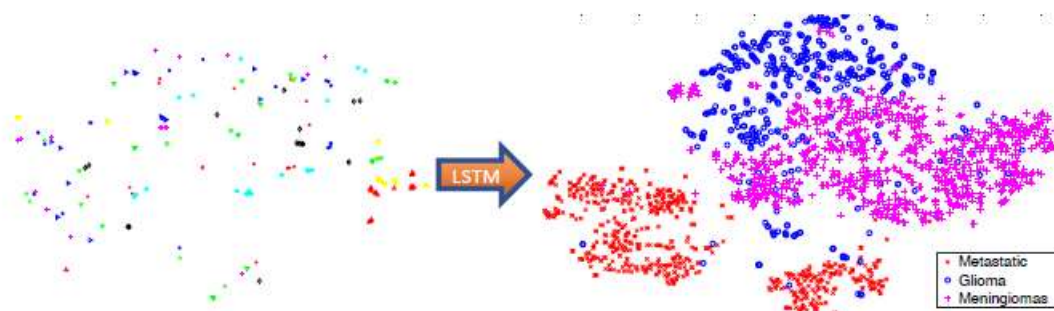


Fig. 7. Quiet embeddings with DenseNet yield (left) and LSTM yield (right). Casing savvy understanding embeddings (demonstrates few patients for simplicity of permeability) in the component extraction arrange (left) are not well-detachable; though they are well-distinct after learning with LSTM.

The mark data; along these lines, the patients are not anticipated that would be distinct from the typical individuals. Fig. 8 outlines the comparing highlight embeddings utilizing tSNE [11]. We can see that while patients are not different in the auto-encoder-include space, they are exceptionally detachable in the element space learned by LSTM.

5 CONCLUSION

In this paper, we exhibited an elective methodology for screening and ordering the cerebrum tumors utilizing all-encompassing 3D MR pictures. Our method is fit for using 3D grouping pictures and does not require the pixel-wise or cut savvy naming. Trials on open and restrictive datasets show that our approach is compelling and very proficient. As future work, we plan to 1) grow our limited dataset for more kinds of mind tumors, and 2) give demonstrate interpretability dependent on feebly administered pathology confinement.

REFERENCES

1. Brian tumor statistics. <http://www.abta.org/about-us/news/brain-tumor-statistics/>. Accessed: 2018-02-16.
2. P. Afshar, A. Mohammadi, and K. N. Plataniotis. Brain tumor type classification via capsule networks. arXiv preprint arXiv:1802.10200, 2018.
3. S. Bauer, L.-P. Nolte and M. Reyes. Fully automatic segmentation of brain tumor images using support vector machine classification in combination with hierarchical conditional random field regularization. In International Conference on Medical Image Computing and Computer-Assisted Intervention, pages 354–361. Springer, 2011.
4. S. Bauer, R. Wiest, L.-P. Nolte and M. Reyes. A survey of MRI-based medical image analysis for brain tumor studies. *Physics in Medicine & Biology*, 58(13): R97, 2013.
5. J. Cheng, W. Huang, S. Cao, R. Yang, W. Yang, Z. Yun, Z. Wang and Q. Feng. Enhanced performance of brain tumor classification via tumor region augmentation and partition. *PloS one*, 10(10):e0140381, 2015.
6. E.-S. A. El-Dahshan, H. M. Mohsen, K. Revett, and A.-B. M. Salem. Computer-aided diagnosis of human brain tumor through MRI: A survey and a new algorithm. *Expert systems with Applications*, 41(11):5526–5545, 2014.
7. M. Havaei, A. Davy, D. Warde-Farley, A. Biard, A. Courville, Y. Bengio, C. Pal, P.-M. Jodoin and H. Larochelle. Brain tumor segmentation with deep neural networks. *Medical image analysis*, 35:18–31, 2017.
8. S. Hochreiter and J. Schmidhuber. Long short-term memory. *Neural Computation*, 9(8):1735–1780, 1997.
9. G. Huang, Z. Liu, L. van der Maaten, and K. Q. Weinberger. Densely connected convolutional networks. In 2017 IEEE Conference on Computer Vision and Pattern Recognition (CVPR), pages 2261–2269. IEEE, 2017.

10. B. H. Menze, A. Jakab, S. Bauer, J. Kalpathy-Cramer, K. Farahani, J. Kirby, Y. Burren, N. Porz, J. Slotboom, R. Wiest, et al. The multimodal brain tumor image segmentation benchmark (BRATS). *IEEE transactions on medical imaging*, 34(10):1993–2024, 2015.
11. L. van der Maaten and G. Hinton. Visualizing high-dimensional data using t-SNE. *Journal of Machine Learning Research*, 9(Nov):2579–2605, 2008.
12. Y. Zhang, D. Shen, G. Wang, Z. Gan, R. Henao, and L. Carin. Deconvolutional paragraph representation learning. In *Advances in Neural Information Processing Systems*, pages 4169–4179, 2017.